

AUTOMATIC IDENTIFICATION OF BUILDING FEATURES FOR SEISMIC DAMAGE ASSESSMENT ON A LARGE SCALE

Pietro Carpanese¹, Marco Donà¹, Francesca da Porto¹

¹ Department of Geosciences, University of Padova
Via G. Gradenigo, 6 – 35131, Padova
e-mail: {pietro.carpanese,marco.dona.1,francesca.daporto}@unipd.it

Abstract

Seismic risk assessment represents a big challenge in countries with a high seismic hazard and a significantly vulnerable built heritage, such as Italy. When carrying out seismic risk evaluations at large scales, however, the identification of buildings and their features can be very costly and time consuming.

In this work, artificial intelligence techniques are used to automatically and remotely retrieve exposure information. First, building data are collected using satellite imagery, then street-view pictures are extracted for each building and Convolutional Neural Networks are trained to recognize specific features of interest, especially those that affect seismic vulnerability. Furthermore, a seismic damage calculation platform is developed.

The results provided by this algorithm can be useful for managing emergencies and establishing priority criteria for seismic mitigation strategies.

Keywords: seismic damage assessment, large-scale analysis, street view images, convolutional neural networks, damage calculation platform

1 INTRODUCTION

Italy is one of the European countries with the highest seismic activity, which caused around 160,000 victims in the last two centuries [1]. Over the last 50 years, earthquakes forced the Italian country to sustain emergency management, recovery and reconstruction costs amounting to around 180 billion euros. For these reasons, seismic risk assessment at large scales plays a crucial role in emergency planning and mitigation policies [2].

Despite the considerable progress that has been made towards more accurate seismic risk assessments, risk management institutions often do not have detailed information that can lead to adequate evaluations. In particular, when conducting large-scale analyses, the assessment of exposure often relies on public data available at the municipal, regional, or national level (e.g., ISTAT census data, cadastral data, etc.), which are often incomplete or inaccurate. On the other hand, a more appropriate estimate of exposure may be hampered by slow and expensive surveys which are necessary to collect a considerable volume of data [3, 4]. Furthermore, even when exposure is properly estimated, the heterogeneity of residential building typologies makes it non-trivial to estimate their vulnerability [5, 6]. This work therefore addresses the issue of faster and more accurate seismic risk assessments at a large scale. The objective of this work is indeed to develop a systematic methodology that can lead to seismic risk assessments on a territorial scale. To accomplish this task, a risk calculation algorithm is implemented: the algorithm is intended to work remotely, which means that no direct on-site investigation of the area is required, and it is also meant to work automatically, which means that seismic risk assessments can be produced for any location in Italy without the need for manual input during the calculation steps.

Particularly, the distribution of buildings in the area of interest is detected through satellite images. This procedure is possible thanks to tools such as OpenStreetMap (OSM), which has already been used and proved useful in previous studies [7-10]. Their typologies are then identified on the basis of street view images. In fact, modern technologies such as Google street View (GSV) allow us to easily retrieve street views of buildings, simulating the external survey of an urban area [11-14]. Based on the collected images, machine learning techniques (in particular, Convolutional Neural Networks [15]) are used to identify specific features of buildings so that they can be associated with their vulnerability level. Finally, a seismic risk calculation platform is developed to perform damage assessments for different seismic scenarios. The outputs generated by the platform can respond to the needs mentioned above, as they provide a solid basis for improving preparedness and planning mitigation measures at a large scale.

2 AUTOMATIC FEATURE RECOGNITION

The first part of this work consists of the simulation of an external survey of buildings carried out at a territorial scale, using tools such as OSM, GSV, and machine learning techniques.

Firstly, OSM was used to retrieve building footprints given a specific satellite image. Other data provided by OSM maps are building centroids and areas, as well as the labels that identify the building typology (such as “apartments”, “detached”, “house”, just to give a few examples). Subsequently, GSV can be leveraged to obtain the street view pictures of all the buildings detected in the area of interest. This operation is possible knowing the building centroids (in terms of latitude and longitude) previously retrieved through OSM. Parameters that define the angle of the street view image, such as heading and pitch, are set so that the best picture of the building is selected (i.e., the picture that shows the best view of the whole façade). Street view pictures can be easily and quickly acquired for all the buildings selected. An example of this procedure is shown in Figure 1: Figure 1(a) shows the satellite image of an area in Pordenone (Friuli Venezia Giulia, North East of Italy), Figure 1 (b) shows the building footprints detected through

OSM with their labels, and lastly Figure 1(c) shows the street view images that were acquired for some of those buildings.

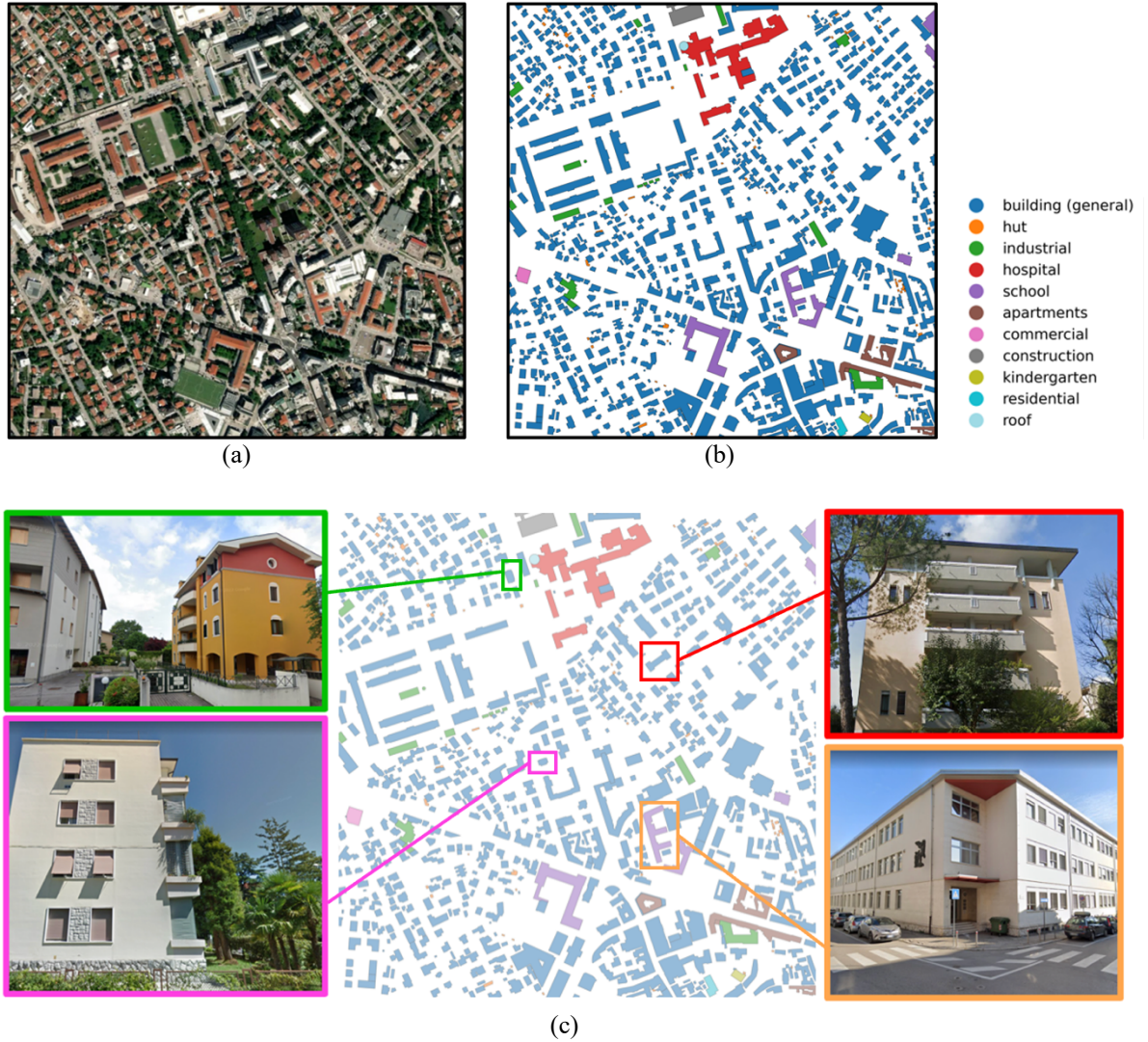


Figure 1: (a) Satellite image of a case study area in the town of Pordenone, (b) OSM map and building labels, (c) examples of street view images retrieved with GSV.

Now that the building footprints are collected, as well as their geographical information and street view pictures, these data can be used to generate even more knowledge about the buildings themselves. Particularly, façade photos can be very helpful in recognizing building features that can be detected from an external survey, such as height, material, and an estimation of the construction period. In order to do so in an automatic way, a machine learning technique was exploited. Specifically, Convolutional Neural Networks (CNNs) were considered. CNNs are deep learning algorithms that are able to take an input image, assign weights and biases to different objects in the image, and distinguish them in order to classify the image itself. A CNN usually consists of three types of layers: convolutional layers, where a dot product between the image and a filter (or kernel) is performed; pooling layers, which decrease the size of the convolved image to reduce the computational costs; and lastly fully connected layers, usually placed before the output layer, which connects the neurons between two different layers.

In order to train a CNN to recognize specific features in images, a database of pictures needs to be created. For the aim of this work, images of Italian residential buildings were gathered

and labeled according to height, material, and construction period (i.e., the three features that need to be predicted). An *ad hoc* dataset was created, collecting pictures from the CARTIS database [16], the Da.D.O. database [17], and from other surveys carried out in the past from the research group of the University of Padova [18]. These sources were used since they all contain a significant and reliable database of building pictures that are already labeled according to height, material, and construction period. Furthermore, data augmentation techniques have been used: this is a common approach in image processing applications since it creates variations of images that can improve the network's ability to recognize new images. These operations allowed the gathering of a total number of 10.000 labeled images, thus making a robust database on which the CNNs could be trained.

Not all the pictures collected in the dataset are actually used for the training of the CNNs. Some of the pictures are kept for the processes of validation and evaluation. As a matter of fact, the training set is the set of data that is used to train the model so that it can learn features and patterns in the data, while the validation set is another dataset that is used to validate the model performance during training, and the evaluation set is used to test the model after training is complete. In Table 1 the number of images for each feature and each class are reported, showing the subdivision into training, validation, and evaluation.

Feature	Labels	Training	Validation	Evaluation	Total
Height	Low-Rise	4,004	856	856	10,000
	Mid-Rise	2,998	643	643	
Material	Masonry	4,906	1,051	1,051	10,000
	R.C.	2,094	449	449	
Construction period	Pre-1919	1,621	348	348	10,000
	1919-1945	510	109	109	
	1946-1960	2,056	440	440	
	1961-1980	1,826	391	391	
	Post 1980	989	211	211	

Table 1: Splitting of images into training, validation, and evaluation sets for height, material, and construction period.

The categories on which the CNNs are trained are the following: for the height parameter, buildings can be classified as LowRise (1-2 storeys) or MidRise (3 or more storeys); for material, the classes are masonry or reinforced concrete (R.C.); for what concerns the construction period, the possible predictions are Pre 1919, 1919-1945, 1946-1960, 1961-1980, and Post 1980. These classifications are consistent with the categories proposed by ISTAT.

After creating the image dataset, the actual training process can begin. Three algorithms were developed, one for each of the parameters that need to be recognized, using the Transfer Learning technique and fine-tuning it. Transfer Learning corresponds to a "network operation": the last set of fully connected layers of a pre-trained CNN is removed and the head is replaced by a new set of fully connected layers with random initializations. This operation has the great advantage of making use of CNNs that are pre-trained on a very large dataset, and then using the CNN either as an initialization or a feature extractor for the task of interest.

More precisely, in this work a CNN is first pre-trained on ImageNet, although the fully connected nodes at the end are removed (i.e., where the actual predictions for the class label are made). These fully connected nodes are then replaced with initialized nodes, while the earlier convolutional layers remained frozen to ensure that all features already learned by the CNN were not deleted. With this new configuration, only the new fully connected layers located in

the head of the CNN are trained. Finally, the convolutional layers are unfrozen again and another training process is performed.

After the training process is completed, the parameters of precision, recall, and F_1 -score can be evaluated. Precision represents number of instances that are relevant out of the total instances the model retrieved, recall is the number of instances which the model correctly identified as relevant out of the total relevant instances, and lastly the F_1 -score combines precision and recall into a single metric by calculating their harmonic mean. The CNNs that were trained for the features “height” and “material” show a good degree of accuracy (F_1 -score greater than 0.85 for all the labels considered), while the performance of the CNN that was trained to recognize the construction period appears to fall short, especially for the 1919-1945 and Post-1980 classes. This is mainly due to the lower number of images belonging to these two categories used to train the CNN (as can be seen in Table 1).

Now that the three CNNs are trained and fine-tuned on the dataset and their specific weights are obtained, they can be used to predict the height, material, and construction period of buildings from new images on which they have not been already trained. The image to be analyzed must be loaded and preprocessed so that it is comparable to the images in the dataset. Subsequently, the algorithm recalls the model previously trained in order to assign the best prediction to the image. This process can be repeated for all the buildings that belong to the area of interest, whose images were collected through GSV, and for all the three features (height, material, and construction period). Figure 2 shows the predicted class labels for each one of these three parameters for the same area shown in Figure 1.

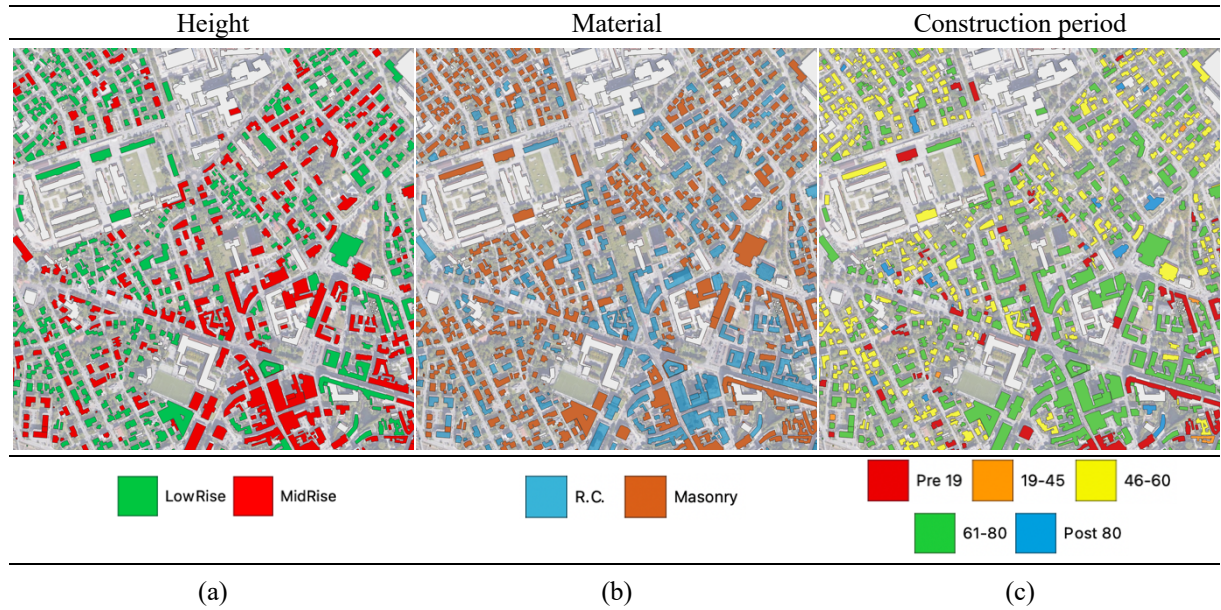


Figure 2: Predictions of height (a), material (b), and construction period (c) for the residential buildings in the area.

In addition to the internal validation of the CNNs, it can be helpful to compare the predictions with data manually gathered through surveys. Since the University of Padova carried out a thorough traditional survey in the Municipality of Pordenone in 2018-2019, that town was chosen as a case study and all the buildings found in Pordenone were analyzed through the algorithm developed here, so that the predictions could then be compared with the information acquired during the manual survey. Figure 3 displays the percentages of accurate and inaccurate predictions made by the three CNNs when compared to the direct survey for the three features

taken into account. Figure 3 shows that for material and height there is an excellent match between CNN predictions and on-site survey results, however this relationship appears to worsen for the feature construction period. Nonetheless, it may be useful to analyze the mismatch in terms of number of classes for the construction period (i.e., how many classes the algorithm fails by). This is more relevant given that the work's ultimate goal is to assess seismic risk at a large scale. As a matter of fact, a mistake of just one class will not affect the results as much as an error of three or four classes might do. The number of epochs deviating from the actual label is differentiated in Figure 4, which shows the right predictions versus the incorrect predictions for the parameter "construction period" in the municipality of Pordenone. As can be seen, the "1 epoch difference" error accounts for more than the half of all incorrect predictions (that 44% in Figure 3). This is a promising outcome since it shows that even when a building is incorrectly identified by the CNN, it usually still correlates it with a construction period that does not significantly alter the taxonomy of the area.

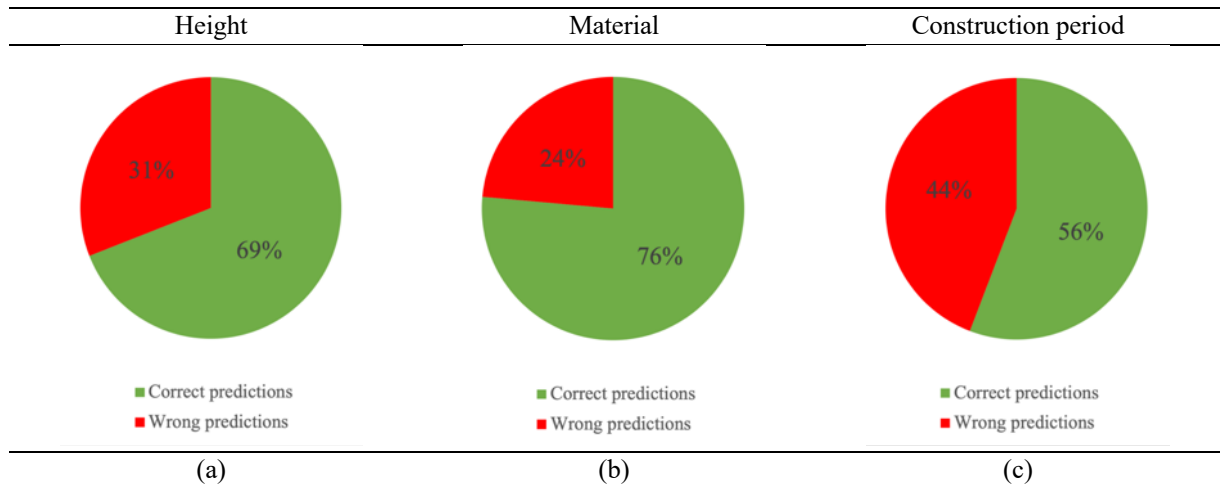


Figure 3: Percentages of correct and wrong predictions for height (a), material (b), and construction period (c) in Pordenone, when compared to the direct survey.

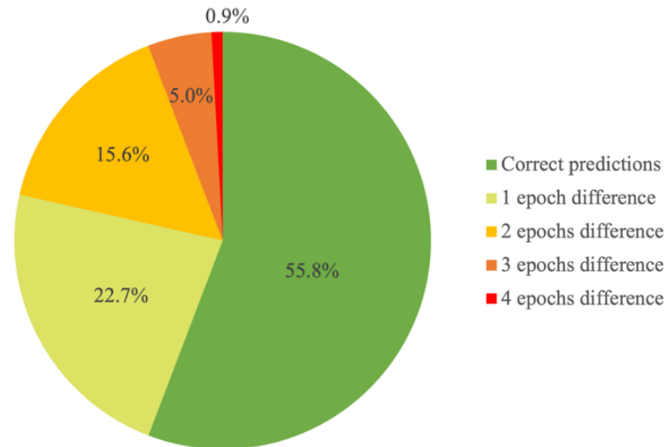


Figure 4: Percentages of correct predictions for construction period and predictions with 1, 2, 3, or 4 epochs difference for Pordenone, when compared to the direct survey

Furthermore, it is important to emphasize how much time can be saved by using this procedure. The was able to automatically analyze satellite pictures of the municipality of Pordenone, extract Google Street View photographs of each building (for more than 8,000 residential

buildings), and classify them according to height, material, and construction period in about two hours. This is a remarkable achievement, especially when compared with time-consuming and expensive traditional surveys.

3 REMOTE SEISMIC DAMAGE ASSESSMENT

After having developed an algorithm that automatically and remotely retrieves information about building taxonomy and exposure, it is possible to use these data to carry out seismic risk assessments. In order to do so, a seismic risk calculation platform has been developed, combining three main modules: the exposure module (where the procedure described in the previous section is implemented), the seismic hazard module and the seismic vulnerability one.

For what concerns seismic hazard, the platform deploys the Italian Seismic Hazard map (MPS04) developed by the *Istituto Nazionale di Geofisica e Vulcanologia* (INGV) and adopted in Italy at national level with the Civil Protection Ordinance OPCM 3519/2006 [19]. It is the official Italian hazard model [20] and it provides the seismic action for 10,751 points of a mesh of 5×5 km covering all the Italian territory, taking into consideration nine return periods ($T_r = 30, 50, 72, 101, 140, 201, 475, 975, 2475$ years). The platform is able to produce seismic maps both in terms of conditional or unconditional damage. Conditional damage expresses the expected damage for a selected return period (in this case, for a specific PGA), while unconditional damage takes into account an observation time window, where the PGA values associated to all the return periods are calculated considering the annual probability of reaching those levels [21]. Moreover, information about the soil type are implemented. Specifically, the platform includes the results provided by Forte et al. [22], which give a percentage of the different types of soils for each Italian municipality. This additional information is indeed essential to calculate the possible amplification of ground motion due to soil characteristics.

The seismic vulnerability module assigns a specific fragility model to each building. These models are often expressed by fragility curves that correlate seismic intensity parameters (e.g., PGA) with the probabilities of exceeding damage states (DSs). Numerous methods for elaborating fragility curves can be found in the literature [23]: in this specific study, the mechanics-based fragility curves proposed by Donà et al. [24] are used to define the vulnerability of masonry buildings, while the empirical fragility curves determined by Rosti et al. [25] are assigned to reinforced concrete buildings. These works propose fragility models for Italian building macro-typologies defined by characteristics such as height and construction period. These are indeed the parameters that the CNNs are trained to recognize in the street view images of buildings. Therefore, the vulnerability module has the task of assigning the appropriate fragility set (from the literature) to each detected building based on its material, height, and construction period.

By combining the hazard module and the vulnerability module, it is possible to calculate the probability of occurrence for each damage state. In this way, it is possible to estimate the probability that a building suffers a given damage state in the event of an earthquake of a certain magnitude. This process is repeated for all the buildings that can be assigned to a fragility set (i.e., for which the material, height, and construction time parameters can be predicted). The average damage can also be calculated from the probability values of the individual damage states, as follows:

$$DS_M = \sum_{i=1}^5 i \cdot DS_i \quad (1)$$

where DS_M is indeed the average damage and DS_i represents the probability of occurrence of a damage state. Each damage state is then multiplied by a coefficient i , ranging from 1 (light

damage) to 5 (complete collapse). This indicator provides a synthetic representation of damage, suggesting the average damage that a building would suffer following an earthquake.

4 RESULTS

The platform described in Section 3 can be used to produce damage maps, which express the probability of buildings of reaching or exceeding the different DSs. Conditional or unconditional damage maps were elaborated in this study: the first ones take into account a specific T_r , while the latter are calculated for an observation time window.

The results for the same area shown in Figure 1 are presented in Figure 5 for conditional damage ($T_r=475$ years) and in Figure 6 for unconditional damage (50 year time window). In both cases, the maps show the probability of reaching or exceeding the damage states DS1, DS3, and DS5.

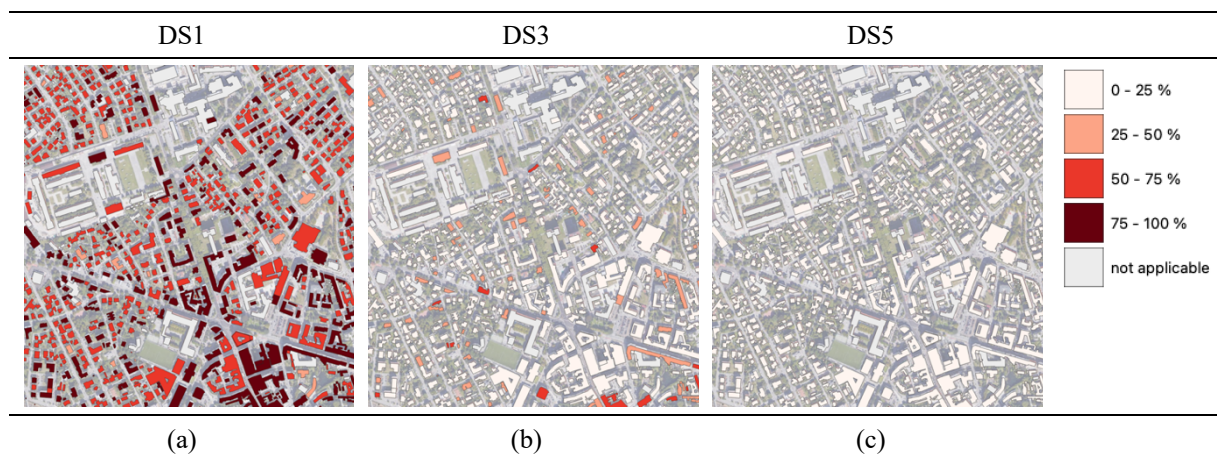


Figure 5: Damage maps DS1 (a), DS3 (b), and DS5 (c) for a return period T_r of 745 years

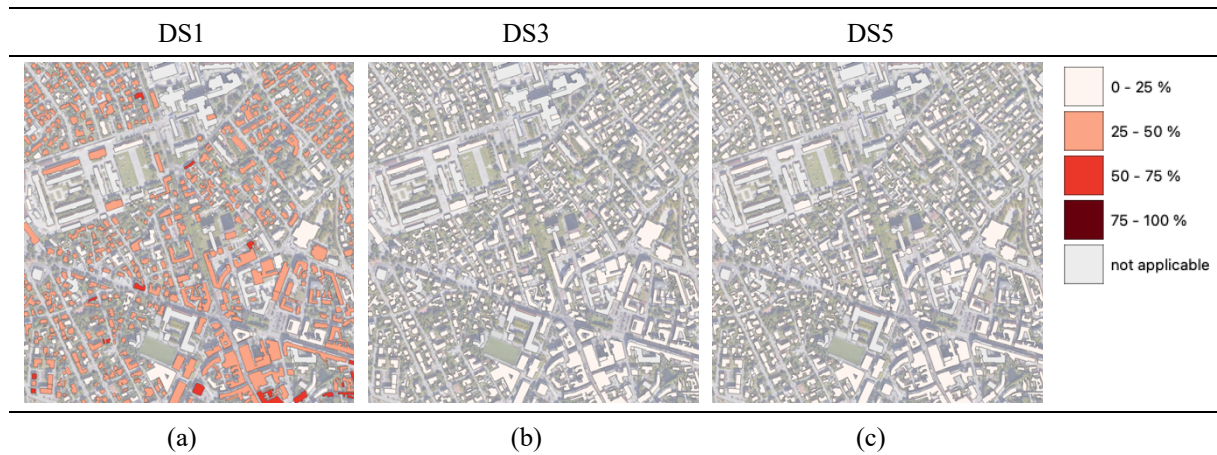


Figure 6: Damage maps DS1 (a), DS3 (b), and DS5 (c) for a time window of 50 years

As can be seen in Figure 5, for a scenario with a T_r of 475 years, most buildings in the area have a probability of more than 50% of reaching a DS1, including a significant number of buildings that have a probability of more than 75% of reaching that damage state. The configuration of the area is indeed heterogeneous and has many buildings with significant vulnerability. As for the maps related to DS3, it is still possible to identify some buildings that reach this damage state with a probability higher than 25%, and very few of them exceed 50%. In the

DS5 maps, no building seems to have a collapse probability higher than 25%. Similar observations can be made about the maps shown in Figure 6.

Lastly, Figure 7(a) and Figure 7(b) show the maps that express the average damage calculated with Equation (1). Most of the buildings are likely to reach a damage equal to DS2 (moderate damage), despite a considerable amount of buildings associated to an average damage of DS1 and DS3.

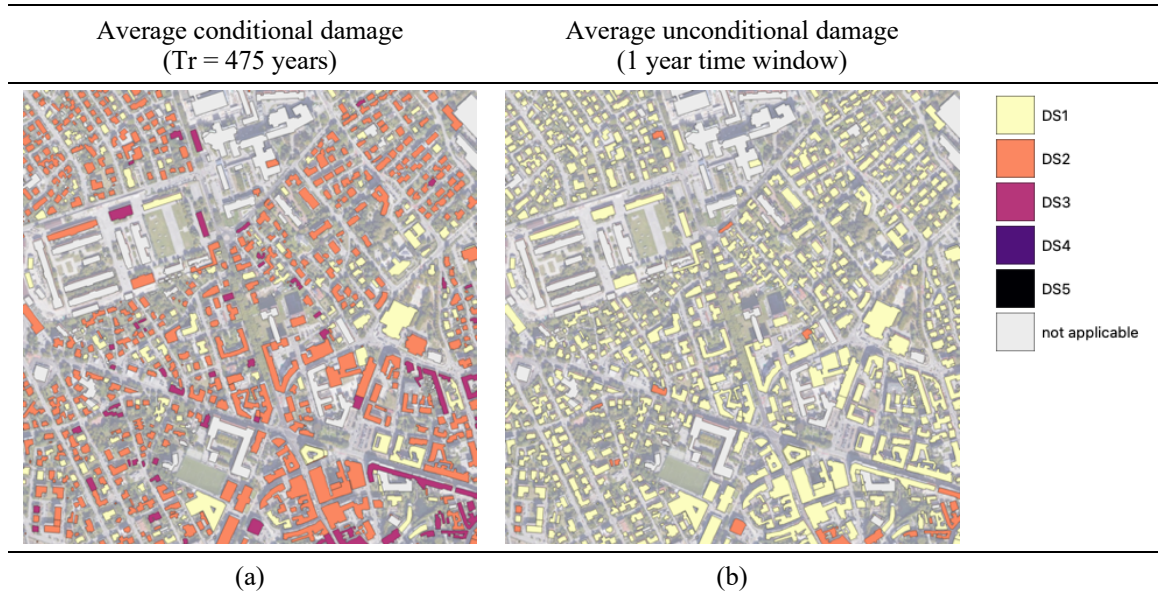


Figure 7: Average damage map for a return period of 475 years (a) and a time window of 50 years (b)

5 CONCLUSIONS

- An algorithm to automatically retrieve building footprints from satellite images has been developed. The algorithm leverages the OSM tool, which also provides additional information such as building centroids, floor areas, and labels that identify the building typology.
- Subsequently, for each building that was detected in the area of interest, a Google Street View image was retrieved, thus simulating an external survey of the area.
- Street view photos have then been used to recognize specific building features, particularly height, material, and construction period. Three CNNs were therefore trained on a dataset of 10,000 labeled images of buildings, so that they could identify the three parameters mentioned above. A validation of the CNNs outputs has been presented to highlight the accuracy of the predictions. This operation is very useful for estimating the exposure of the area under consideration and for associating the correct vulnerability to each building.
- A seismic risk calculation platform has been developed, including modules of seismic hazard, vulnerability and exposure that eventually provide seismic damage estimates. Some possible results in terms of damage maps have been presented, which show the probability of reaching or exceeding specific damage states for different seismic scenarios, as well as a synthetic index to indicate the average damage.
- The methodology developed in this work can be a useful tool for disaster management institutions, insurance companies and any other organization dealing with risk management. The algorithm developed in this work can not only assess seismic damage for specific earthquake scenarios, but it also has the ability to make predictions and projections

over different time windows. These results can give important indications on how many human and economic resources are expected to be deployed for different scenarios, which is something that is typically not known by the agencies mentioned above. Lastly, the platform can support authorities in the selection of effective mitigation strategies and recovery plans.

- This work leaves room to further developments, such as the implementation of consequence matrices to compute seismic risk indicators (e.g., economic losses, casualties, etc.) starting from the seismic damage maps shown here. In addition, other neural networks could be developed to detect additional building features, especially those that affect their seismic vulnerability. The same process could be implemented for other building typologies so that specific features relevant to defining their seismic vulnerability are detected.

REFERENCES

- [1] DPC - Italian Civil Protection Department of the Presidency of the Council of Ministers (2018). National risk assessment - Overview of the potential major disasters in Italy, seismic, volcanic, tsunami, hydro-geological/hydraulic and extreme weather, droughts and forest fire risks, 2018.
- [2] United Nations International Strategy for Disaster Reduction, Sendai Framework for Disaster Risk Reduction 2015-2030. https://www.unisdr.org/files/43291_sendaiframeworkfordrren.pdf, 2015
- [3] M. Polese, M. Di Ludovico, A. Prota, G. Tocchi, M. Gaetani d'Aragona, M. Utilizzo della scheda Cartis per aggiornamento dell'inventario ed effetto sulle stime di vulnerabilità a scala territoriale. *Proceedings of the 'XVIII Convegno Nazionale di Ingegneria Sismica' (XVIII ANIDIS)*. Ascoli Piceno, Italy, September 15-19, 2019. (in Italian)
- [4] L. Sbrogio, Y. Saretta, F. Molinari, M. R. Valluzzi. Multilevel assessment of seismic damage and vulnerability of masonry buildings (MUSE-DV) in historical centers: development of a mobile android application, *Sustainability*, **14**(12), 7145, 2022.
- [5] M. Dolce, A. Prota, B. Borzi, F. da Porto, S. Lagomarsino, G. Magenes, C. Moroni, A. Penna, M. Polese, E. Speranza, G. M. Verderame, G. Zuccaro, Seismic risk assessment of residential buildings in Italy, *Bulletin of Earthquake Engineering*, **19**(8), 2999–3032, 2021.
- [6] F. da Porto, M. Donà, A. Rosti, M. Rota, S. Lagomarsino, S. Cattari, B. Borzi, M. Onida, D. De Gregorio, F.L. Perelli, C. Del Gaudio, P. Ricci, E. Speranza, Comparative analysis of the fragility curves for Italian residential masonry and RC buildings, *Bulletin of Earthquake Engineering*, **19**(8), 3209–3252, 2021.
- [7] F. Biljecki, H. Ledoux, J. Stoter, Generating 3D city models without elevation data, *Computers, Environment and Urban Systems*, **64**, 1-18, 2017.
- [8] M. Fleischmann, A. Feliciotti, O. Romice, S. Porta, Morphological tessellation as a way of partitioning space: Improving consistency in urban morphology at the plot scale. *Computers, Environment and Urban Systems*, **80**, 101441, 2020.
- [9] M. Pittore, M. Wieland, Toward a rapid probabilistic seismic vulnerability assessment using satellite and ground-based remote sensing, *Natural Hazards*, **68**(1), 115–145, 2013.

- [10] R. Hecht, G. Meinel, M. Buchroithner. Automatic identification of building types based on topographic databases—a comparison of different data sources. *International Journal of Cartography*, **1**(1), 18–31, 2015.
- [11] C. Wang, Q. Yu, K. H. Law, F. McKenna, S. Yu, E. Taciroglu, A. Zsarnóczy, W. Elhaddad, B. Cetiner, Machine learning-based regional scale intelligent modeling of building information for natural hazard risk management, *Automation in Construction*, **122**, 2021.
- [12] F. Zhang, B. Zhou, L. Liu, Y. Liu, H. H. Fung, H. Lin, H., C. Ratti, Measuring human perceptions of a large-scale urban region using machine learning, *Landscape and Urban Planning*, **180**, 148–160, 2018.
- [13] Y. Yan, B. Huang, Estimation of building height using a single street view image via deep neural networks, *ISPRS Journal of Photogrammetry and Remote Sensing*, **192**, 83–98, 2022.
- [14] J. Kang, M. Körner, Y. Wang, H. Taubenböck, X. X. Zhu. Building instance classification using street view images. *ISPRS Journal of Photogrammetry and Remote Sensing*, **145**, 44–59, 2018.
- [15] K. Simonyan, A. Zisserman. Very deep convolutional networks for large-scale image recognition. *3rd International Conference on Learning Representations, ICLR 2015 - Conference Track Proceedings*, 1–14, San Diego, CA, USA, May 7 - 9, 2015.
- [16] G. Zuccaro, M. Dolce, D. De Gregorio, E. Speranza, C. Moroni, La scheda Cartis per la caratterizzazione tipologico- strutturale dei comparti urbani costituiti da edifici ordinari. Valutazione dell’esposizione in analisi di rischio sismico. *GNGTS 2015*, Trieste, Italy, November 17–19, 2015. (in Italian)
- [17] M. Dolce, E. Speranza, F. Giordano, B. Borzi, F. Bocchi, C. Conte, A. Di Meo, M. Faravelli, V. Pascale, Observed damage database of past Italian earthquakes, The Da.D.O. WebGIS, *Bollettino Di Geofisica Teorica Ed Applicata*, **60**(2), 141–164, 2019.
- [18] M. Vettore, M. Donà, P. Carpanese, V. Follador, F. da Porto, M.R. Valluzzi, A multilevel procedure at urban scale to assess the vulnerability and the exposure of residential masonry buildings, the case study of Pordenone, Northeast Italy, *Heritage*, **3**(4), 1433–1468, 2020.
- [19] OPCM 3274/2003, Primi elementi in materia di criteri generali per la classificazione sismica del territorio nazionale e di normative tecniche per le costruzioni in zona sismica (in Italian). Off. Gazzette Ital. Repub. N°105 8th May 2003.
- [20] M. Stucchi, C. Meletti, V. Montaldo, H. Crowley, G. M. Calvi, E. Boschi, Seismic hazard assessment (2003–2009) for the Italian building code, *Bulletin of the Seismological Society of America*, **101**(4), 1885–1911, 2011.
- [21] B. Borzi, M. Onida, M. Faravelli, D. Polli, M. Pagano, D. Quaroni, A. Cantoni, E. Speranza, C. Moroni, IRMA platform for the calculation of damages and risks of Italian residential buildings, *Bulletin of Earthquake Engineering*, **19**(8), 3033–3055, 2021.
- [22] G. Forte, E. Chioccarelli, M. De Falco, P. Cito, A. Santo, I. Iervolino, Seismic soil classification of Italy based on surface geology and shear-wave velocity measurements, *Soil Dynamics and Earthquake Engineering*, **122**, 79–93, 2019.

- [23] G.M., Calvi, R. Pinho, G. Magenes, J. J. Bommer, L. F. Restrepo-Vélez, H. Crowley, Development of seismic vulnerability assessment methodologies over the past 30 years, *ISET Journal of Earthquake Technology*, **43**(3), 75-104, 2006.
- [24] M. Donà, P. Carpanese, V. Follador, L. Sbrogiò, F. da Porto, Mechanics-based fragility curves for Italian residential URM buildings, *Bulletin of Earthquake Engineering*, **19**(8), 3099–3127, 2021.
- [25] A. Rosti, C. Del Gaudio, M. Rota, P. Ricci, M. Di Ludovico, A. Penna, G. M. Verderame, Empirical fragility curves for Italian residential RC buildings, *Bulletin of Earthquake Engineering*, **19**(8), 3165–3183, 2021.